

Peptide Diffusion and Self-Assembly in Ambient Water Nanofilm on Mica Surface

Hai Li,^{*,†} Feng Zhang,^{#,†} Yi Zhang,^{*,†} Ming Ye,^{†,‡} Bo Zhou,^{†,‡} Yu-Zhao Tang,[§] Hai-Jun Yang,^{†,‡} Mu-Yun Xie,^{†,‡} Sheng-Fu Chen,^{||} Jian-Hua He,[†] Hai-Ping Fang,[†] and Jun Hu^{*,†,§,⊥}

Shanghai Institute of Applied Physics, Chinese Academy of Sciences, Shanghai 201800, China, Graduate School of the Chinese Academy of Sciences, Beijing 100049, China, Bio-X Life Sciences Research Center, College of Life Science and Biotechnology, Shanghai JiaoTong University, Shanghai 200240, China, Institute of Pharmaceutical Engineering, College of Materials Science and Chemical Engineering, Zhejiang University, Zhejiang 310027, China, and Shanghai Center for Systems Biomedicine, Shanghai 200240, China

Received: April 15, 2009; Revised Manuscript Received: May 27, 2009

Ambient water nanofilms confined on solid surfaces usually show properties not seen in bulk and play unique roles in many important processes. Here we report diffusion and self-assembly of peptides in ambient water nanofilms on mica, based on “drying microcontact printing” and ex situ atomic force microscopy imaging. We found that diffusion and self-assembly of several peptides in the water nanofilms on mica resulted in one-dimensional “epitaxial” nanofilaments. The peptide self-assembly process is sensitive to the amount of water on the surface, and different peptides with varied molecular structures show different humidity-dependent behaviors. In addition, some peptides that cannot form nanofilaments on substrates in bulk water can be successfully self-assembled into nanofilaments in the water nanofilm.

1. Introduction

Water confined within nanometer scale usually exhibits interesting phenomena that do not occur in bulk.^{1–8} When a solid is exposed in ambient condition, a water nanofilm will usually be formed. This water nanofilm forms a densely connected two-dimensional (2-D) H-bond network, which is confined between the supporting substrate and the vapor/liquid interface with a thickness from several to hundreds of angstroms which has been found as a function of relative humidity (RH) at a certain temperature.^{1,8,9} The 2-D confined water plays a unique role in many important processes, including surface corrosion, earth evolution, and climate change.^{1,8,10,11}

In 1995, Hu et al. discovered the 2-D water nanofilm on mica surface experimentally by using scanning polarization force microscopy (SPFM).³ They found the formation of metastable, polygon shaped islands, which had an epitaxial relationship with the underlying mica substrate. These islands were hypothesized to be ice-like in nature. Thereafter the structures and properties of ambient water nanofilm on solids have renewed wide attention, both experimentally and theoretically.^{1,8,10–14} The formation of such a water structure with a densely connected 2-D H-bond network was verified by subsequent spectroscopic studies. Sum-frequency generation (SFG) vibrational spectroscopy showed that D₂O on mica adopted a predominately ordered structure and no free OD bonds at the interface of the vapor and adsorbed D₂O layer.¹⁰ Using Fourier transform infrared

(FTIR) spectroscopy, Ewing and Cantrell found that water nanofilms adsorbed on mica exhibited a more structured and rigid H-bond network than that of bulk water.⁹ The first layer of the interfacial water on mica was also confirmed as a 2-D ordered H-bond network by synchrotron X-ray measurements and the ordering decreased with the increased water film thickness.^{15,16} Molecular dynamics (MD) and Monte Carlo simulations of water nanofilms on the mica surface consistent with the experimental data also indicated that the first layer should form a stable, fully connected 2-D H-bond network configuration with no free OH bonds at the interface separating the adsorbed layer and the vapor.^{11,12,14} The ambient water film on the mica surface has also been used as a model system to study many important physical/chemical processes in varied scientific areas.^{1,8,15,17–19} To the best of our knowledge, however, no report has been presented about its effects on a biological process.

Self-assembly of short peptides has been widely used as a biological model system to study protein folding and aggregation.^{20,21} Also, self-assembly of peptides into nanostructures with desired shapes and functionalities provides a route to fabricating new materials and functional devices.^{21–23} Self-assembly of peptides is usually sensitive to many weak interactions and can occur only under certain conditions.^{22–24} These interactions are subtle and very sensitive to the water environment around, especially when the self-assembly happens in a nanoscopic-confined space.^{25,26} In a physically confined environment, it has been shown that the confinement effects can play dominant roles on self-assembly of block copolymers to generate novel structures which are not accessible in the bulk, thus providing opportunities to engineer new structures with potential novel applications.^{25–27}

In our previous study, a peptide named GAV-9 (NH₂–VGGAVVAGV–CONH₂), a conserved consensus of α -synuclein, β -amyloid protein, and prion protein, exhibited one-

* Corresponding authors. Tel: 86-21-39194908. Fax: 86-21-59552394. E-mail: zhangyi@sinap.ac.cn; hujun@sinap.ac.cn.

[†] Shanghai Institute of Applied Physics.

[‡] Graduate School of the Chinese Academy of Sciences.

[§] Shanghai JiaoTong University.

^{||} Zhejiang University.

[⊥] Shanghai Center for Systems Biomedicine.

[#] These authors contributed equally to this work.

dimensional (1-D) "epitaxial" self-assembly behaviors susceptible to the hydrophobicity/hydrophilicity of substrates in bulk solutions, a horizontal orientation on hydrophobic HOPG and an "upright" orientation on hydrophilic mica of the resulted nanofilaments.²³ The water nanofilm on solid surfaces consists of a densely connected 2-D H-bond network, which has less free/dangling OH bond, is thought to have a profound influence on the hydrophilicity/hydrophobicity of the surfaces.^{28,29} On the other hand, it has been reported that the hydrophobic interaction is the most effective molecular driving force in peptide self-assembly.^{22,23,30,31} Thus, it should be interesting to see if the self-assembly of the peptides could happen and new peptide structures would be formed in such a nanoscopic-confined environment. In this paper, we put the peptides in the ambient water nanofilm on mica and found unexpected self-assembly of some peptides, including the peptide GAV-9, into novel one-dimensional epitaxial nanofilaments, based on "drying micro-contact printing" (D- μ CP) and ex situ atomic force microscopy (AFM) imaging.

2. Experimental Section

Peptides Sample Preparation. Peptide GAV-9 (NH_2 -VGGAVVAGV- CONH_2), GAV-9a (CH_3CONH -VGGAVVAGV- CONH_2), and a hydrophilic peptide (H_2N -KNDQRNEQ- CONH_2) were all synthesized by using the Boc solid-phase method on an ABI 433A peptide synthesizer (Applied Biosystems) and cleaved from the MBHA resin (100–200 mesh, Fluka) with hydrogen fluoride. These peptides were purified through a TSK-40 (S) column (2.0 cm \times 98 cm, Tosoh). A- β (1–42) peptide was purchased from Sigma-Aldrich Company. Before use, all peptides were dissolved in Milli-Q water.

Fabrication of Stamps and D- μ CP of Peptides. Polydimethylsiloxane (PDMS) stamps were fabricated by pouring a 10:1 (w:w) mixture of Sylgard 184 elastomer/curing agent (Dow Corning) over a master with 1.6 μm pitch on its surface and heating at 70 $^\circ\text{C}$ for 12 h after degassing. The surface of the PDMS stamp was exposed to the degassed peptides solutions for about 2 min. The excess solution was removed, and then the stamp was dried under a stream of nitrogen gas. After inking, the stamp was brought into contact with freshly cleaved mica, and a very small amount of force was applied to make a better contact between both surfaces. At last, the stamp was removed after about 20 s and the strip-like patterns of peptides were left on the mica. The transfer processes were conducted at 20 $^\circ\text{C}$ and RH of $\sim 40\%$ or less (D- μ CP).

Ambient Water Nanofilm on Mica. The thickness of the adsorbed water layer has been found as a function of the relative humidity and temperature. Thus, we can get ambient water nanofilms with varied thicknesses and structures by controlling the environment temperature and relative humidity. In our experiment, freshly cleaved mica surfaces with the strips of different peptides were incubated in a climatic chamber (SDH-01N, Shanghai Jianheng Instrument Company) at 20 $^\circ\text{C}$ and strictly controlled RH. The RH and temperature were controlled with an accuracy of $\pm 5\%$ and ± 0.1 $^\circ\text{C}$, respectively. In most cases in our experiments, the temperature inside the chamber was lower than that in the environment outside. Since the water is likely to condense onto a cooler surface, tiny water droplets would usually form on the mica surface if we took the sample out from the chamber directly into the ambient condition after the incubation. In order to avoid the formation of water droplets, all of the samples were transferred immediately into a sealed box inside the chamber within several seconds. The sealed box was half filled with dry silica gel to ensure a dry atmosphere

inside it. The samples were kept in the sealed box for tens of minutes before being taken out from the chamber to guarantee a dry sample surface. Then the samples were taken out and kept in the sealed box for about 10 min in the outside room environment for temperature equilibrium before being transferred to the AFM chamber. By doing so, no droplets could be found on the sample surfaces.

Atomic Force Microscopy. A commercial AFM instrument (Nanoscope IIIa, Veeco) equipped with an E-scanner (10 μm \times 10 μm) and a liquid cell was employed. The tapping mode in air was performed to observe the peptide strips on mica and their changing after different incubations, tapping mode in liquids was used to image the peptide assembly on the surfaces in bulk water, and the contact mode was applied to obtain the atomic resolution images of the mica surface. Silicon nitride cantilevers with the normal spring constants of 2–10 N m^{-1} (NSG 11, NT-MDT) and 0.58 N m^{-1} (NPS, Veeco) were used in air and liquid, respectively. All images were captured with a scan rate at 1–2 Hz and 512 \times 512 pixel resolution.

The AFM ex situ imaging was achieved by taking the following procedures: (i) after the initial image was collected the tip was retracted for tens of micrometers; (ii) a transparent clean film was covered and fixed on the screen of monitor coupled with CCD in the AFM system, and the evident characteristics of the sample surface as well as the probe cantilever were delineated on the film by using a water color pen; (iii) before imaging the incubated peptide sample, the remounted sample and the probe cantilever were regulated to superpose the corresponding features recorded on the transparent film; (iv) a relative large scan area (usually within several micrometers) was first imaged and the previous target location could be zoomed in later. In this way, we could easily and precisely relocate the same small area for many times. Ex situ imaging was conducted in air under RH no more than 30% at room temperature.

Attenuated Total Reflection Infrared (ATR-IR). The ATR-IR spectra were taken by using a Bruker EQUINOX 55 Fourier transform infrared spectrometer equipped with a DGTS detector and a ZnSe-window, single-bounce, attenuated total reflectance (ATR) accessory installed into the sample compartment. The ATR-IR spectra were collected by pressing the side with a sample of mica substrate into contact with the ZnSe element. All spectra were obtained at 64 scans and with a resolution of 4 cm^{-1} .

3. Results and Discussion

In the experiment, we employed a D- μ CP process, which guaranteed that only negligible bulk water was present. Ex situ AFM imaging was operated under low RH ($< 30\%$) and could monitor the dynamic evolution of the peptide patterns in the water nanofilm on mica. Below RH 30%, it was found that peptide patterns could hold their status even for several months.

When the peptide pattern on the mica surface was incubated in a high RH environment for a long incubation time, the peptides diffused on the surface and self-assembled into 1-D "epitaxial" nanofilaments under the well-controlled conditions. Typically, GAV-9 started to diffuse and grow into nanofilaments within 60 min at RH 90% and 20 $^\circ\text{C}$ and formed highly ordered "epitaxial" nanofilaments after several hours. Ex situ AFM observation revealed more details of the dynamic evolution of GAV-9 peptide diffusion and self-assembly process in our experiment (Figure 1).³² D- μ CP generated GAV-9 strips (Figure 1a) exhibited a decrease in height (from ~ 0.7 to ~ 0.3 nm) at the beginning of the incubation (Figure 1b), and peptides could

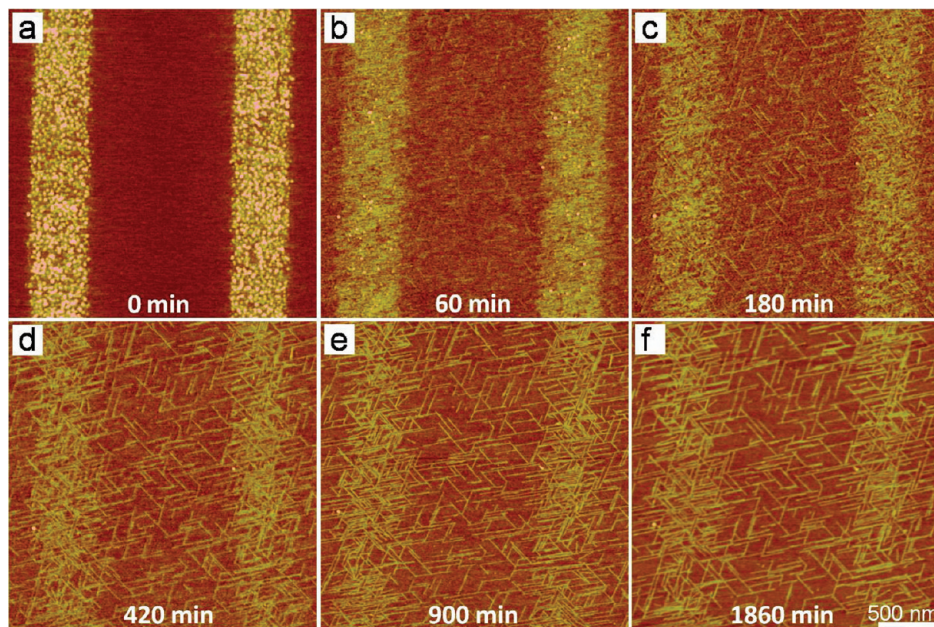


Figure 1. Ex situ AFM observation of GAV-9 diffusing and self-assembly in ambient water nanofilm on mica. (a) D- μ CP-generated GAV-9 strips; (b–f) ex situ tapping-mode AFM images of the strips after incubated at RH 90% and 20 °C for different time periods. The scale bar in (f) applies to all images.

be observed in the gaps between the strips, indicating a diffusion process. Over time, more and more nanofilaments appeared in both the gaps and the initial GAV-9 strips (Figure 1c–e). From 900 to 1860 min, some GAV-9 nanofilaments disassembled, and new nanofilaments formed (Figure 1f), illustrating a dynamic balance between self-assembly and disassembly of peptide molecules.

The “epitaxial” relationship of GAV-9 nanofilaments with the underlying mica lattice has been confirmed by AFM observation in air (Figure 2, panels a and b). In addition, their 3-fold symmetry looks similar to that observed on the mica surface immersed in bulk water.²³ However, the average height of ~ 0.5 nm of the GAV-9 nanofilaments is much lower than the height of nanofilaments (~ 2 nm, Figure S1) formed in bulk experiment,²³ suggesting that the peptide molecules adopts a “lying down” style that the peptide backbone is parallel to the substrate because of the strong interaction with the water nanofilm. From the attenuated total reflection infrared (ATR-IR) spectra (Figure 2c), an absorbance peak at 1627 cm^{-1} with a shoulder peak at higher wavenumber was found on the sample prepared in bulk water, indicating an antiparallel beta-sheet structure,^{21,33} whereas in the sample prepared in the water nanofilm, the peaks shifted slightly and a peak at 1616 cm^{-1} was clearly seen. This shift might be understandable if we consider the subtle and different interactions between the beta-sheet and mica surface since the peptides adopt different orientations on mica from the height measurement of nanofilaments. Interestingly, the nanofilaments that formed in bulk water could disassemble in the ambient water nanofilm, indicating the instability of bulk-fabricated nanofilaments under this ambient condition (see Figure S2). In contrast, the nanofilaments self-assembled in this water nanofilm were much more stable in a wide range of humidity.

The peptide self-assembly seems very sensitive to the amount of water on the surface, and different peptides with varied hydrophobicities show different humidity-dependent behaviors. At humidity lower than 60%, GAV-9 hardly formed nanofilaments, although it could diffuse easily on the surface. There were no obvious differences among the structures of GAV-9

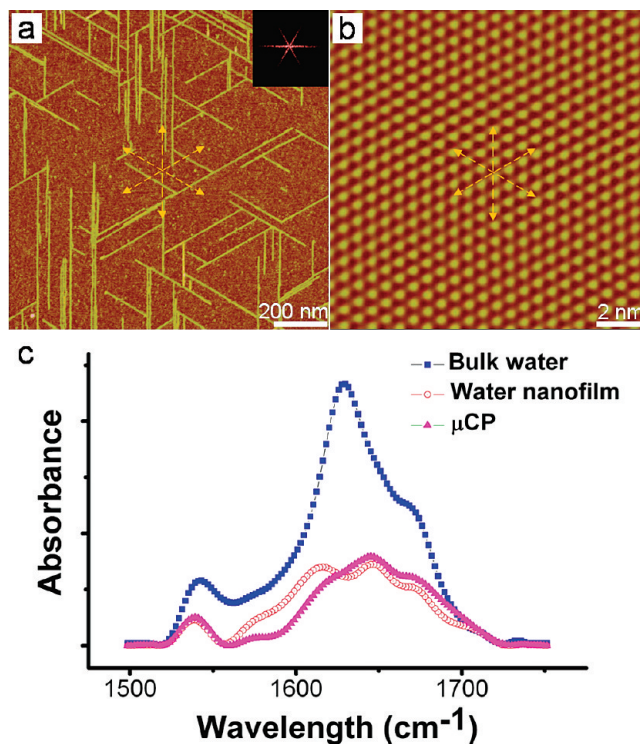


Figure 2. Epitaxial growth of GAV-9 nanofilaments in the ambient water nanofilm on mica. (a) AFM image of GAV-9 nanofilaments grown from D- μ CP-generated strips after incubated; inset is the 2-D Fourier transform. (b) AFM image of the atomic lattice of the underlying mica surface of (a). (c) ATR-IR spectra of GAV-9 samples: Triangle, peptide strips generated by D- μ CP. Circle, GAV-9 nanofilaments grown from D- μ CP-generated strips after incubated in water nanofilm. Square, GAV-9 fibrils grown in bulk water.

nanofilaments grown under RH from 70% to 95%. However, the peptide GAV-9a ($\text{CH}_3\text{CONH-VGGAVVAGV-CONH}_2$ —derived from GAV-9 by replacing the hydrophilic N terminal ($-\text{NH}_2$ group) with the hydrophobic $-\text{NHCOCH}_3$ group) started forming “epitaxial” nanofilaments at a much lower RH 45%, as shown in Figure 3b, where fine “epitaxial” nanofilaments

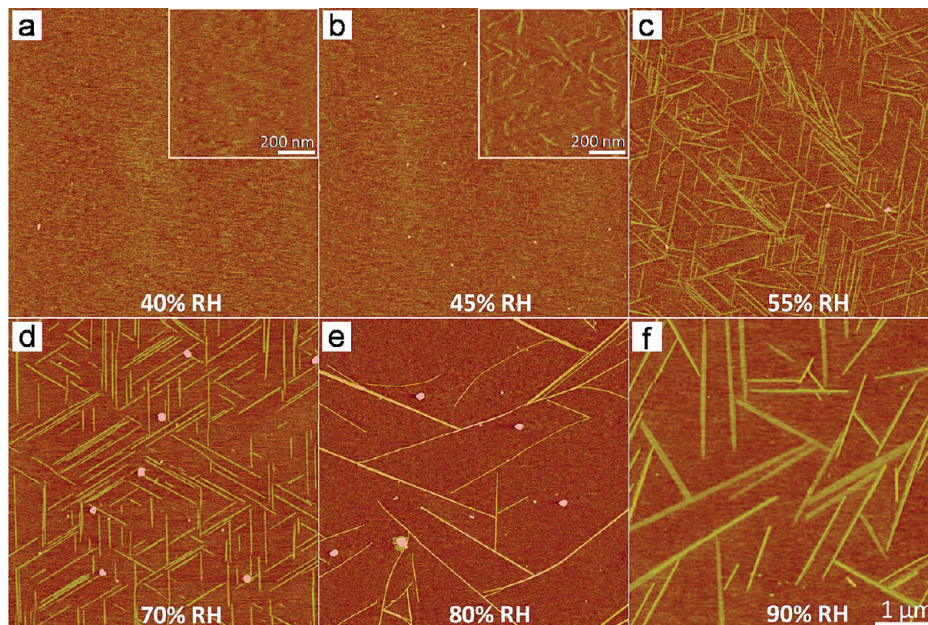


Figure 3. AFM images of self-assembly nanofilaments of GAV-9a in ambient water nanofilm. GAV-9a strips are incubated at (a) RH 40% for 48 h; (b) RH 45% for 34 h; (c) RH 55% for 24 h; (d) RH 70% for 24 h; (e) RH 80% for 24 h; (f) RH 90% for 16 h. Insets in a and b are their megascopic pictures. The scale bar in (f) applies to all images.

could be observed at RH \sim 55–70%. Surprisingly, at RH \sim 70–80%, the “epitaxial” orientation began to shift. At RH \sim 90% or higher, the nanofilaments showed varied orientations.

The observation that the pattern of GAV-9a nanofilaments strongly deviates from the pattern of GAV-9 nanofilaments could possibly be explained by the fact that liquid–vapor water interface is hydrophobic.³⁴ In our system, the hydrophobic GAV-9a molecules orient to maximize exposure of their side chains to the hydrophobic side of the interface. Along with the increase of RH, water nanofilm grows thicker, which leads to a strongly decreased interaction of hydrophobic peptide molecules, attached to the liquid–vapor water interface, with the mica substrate. Therefore, at high RH the GAV-9a nanofilaments show varied orientations. However, this does not occur for GAV-9 peptides, as their hydrophilic terminal groups remain immersed in water nanofilm and can still strongly interact with negatively charged mica surface.

Furthermore, A- β (1–42) peptide, a major species of Alzheimer’s disease,³⁵ exhibited the similar behaviors. Normally, A- β (1–42) cannot form “epitaxial” nanofilaments on mica in bulk water even at a high concentration.³⁵ In our case, however, A- β (1–42) formed “epitaxial” nanofilaments after incubated at RH 90% and 20 °C for 12 h (Figure 4a).

We emphasize here that the ambient water nanofilm on mica also provides an environment for hydrophilic peptides to self-assemble into nanofilament structures, such as the highly hydrophilic peptide (H₂N–KNDQRNEQ–CONH₂) (Figure 4b, 20 °C, RH 90%). Peptide H₂N–KNDQRNEQ–CONH₂ hardly formed nanofilaments on either hydrophilic mica or hydrophobic highly ordered pyrolytic graphite (HOPG) in bulk water, even at a high concentration.

We noted that, below RH 30%, the peptide strips could stay there for weeks and even months without observable diffusion (Figure S3). This was because there was rare water on the mica surface and the adsorbent interactions between peptides and mica was strong and the thermal energy was not sufficient to move the peptide molecules around on the surface. This fact further indicated that it was no other than the water nanofilm which

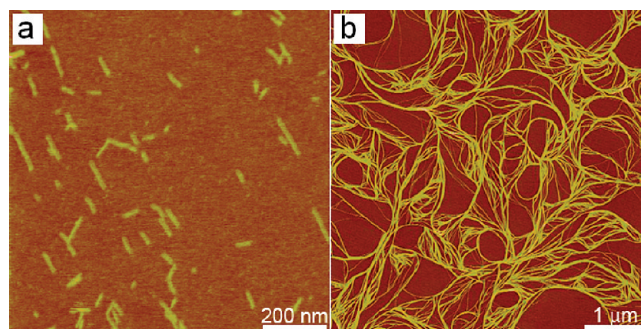


Figure 4. AFM images of nanofilaments of A- β (1–42) and highly hydrophilic peptide H₂N–KNDQRNEQ–CONH₂ self-assembled in ambient water nanofilm on mica. (a) A- β (1–42) forms “epitaxial” nanofilaments after incubated. (b) H₂N–KNDQRNEQ–CONH₂ formed nanofilaments after incubated.

was responsible for the decrease of the adsorbent interactions and then enabled the peptides diffusion.

4. Conclusions

In summary, we have shown diffusion and self-assembly of peptides in ambient water nanofilm with a new type of “lying down” epitaxial structures. It has been found that peptide self-assembly on the surface is sensitive to the environment around. We note that the novel structures and the understanding of the self-assembly mechanism are very important for the fabrication of artificial bionanomaterials and may also be interesting for the relevant medical research.^{21,22,36–38} Generally, the water interface at nanoscale is believed to have a unique function in biological structure and dynamics.^{7,39–41} Particularly, as indicated by Whitesides et al., molecular recognition in the cell, which is the most fundamental process in biochemistry and plays a central role on cell activity, is much more complicated and difficult to understand because the contribution from the confined cell water cannot be ignored.⁴² Since the direct study of the functions of this kind of confined water in vivo in those complicate samples is difficult, we believe that our water system plus MD simulation can be used as a simplified model system

to study the effects of 2-D confined interfacial water on a biological process at the molecular level.

Acknowledgment. We thank Profs. H. Y. Hu and J. C. Li for helpful discussions. This work was supported by grants from Chinese Academy of Sciences, the National Science Foundation of China under Grant No. 30600144, and the National Basic Research Program of China under Grant No. 2007CB936000.

Supporting Information Available: Extensive figures. This material is available free of charge via the Internet at <http://pubs.acs.org>.

References and Notes

- (1) Ewing, G. E. *Chem. Rev.* **2006**, *106*, 1511.
- (2) Gong, X. J.; Li, J. Y.; Lu, H. J.; Wan, R. Z.; Li, J. C.; Hu, J.; Fang, H. P. *Nat. Nanotechnol.* **2007**, *2*, 709.
- (3) Hu, J.; Xiao, X. D.; Ogletree, D. F.; Salmeron, M. *Science* **1995**, *268*, 267.
- (4) Levinger, N. E. *Science* **2002**, *298*, 1722.
- (5) Li, J. Y.; Gong, X. J.; Lu, H. J.; Li, D.; Fang, H. P.; Zhou, R. H. *Proc. Natl. Acad. Sci. U.S.A.* **2007**, *104*, 3687.
- (6) Major, R. C.; Houston, J. E.; McGrath, M. J.; Siepmann, J. I.; Zhu, X. Y. *Phys. Rev. Lett.* **2006**, *96*, 177803.
- (7) Pal, S. K.; Zewail, A. H. *Chem. Rev.* **2004**, *104*, 2099.
- (8) Verdaguer, A.; Sacha, G. M.; Bluhm, H.; Salmeron, M. *Chem. Rev.* **2006**, *106*, 1478.
- (9) Cantrell, W.; Ewing, G. E. *J. Phys. Chem. B* **2001**, *105*, 5434.
- (10) Miranda, P. B.; Xu, L.; Shen, Y. R.; Salmeron, M. *Phys. Rev. Lett.* **1998**, *81*, 5876.
- (11) Odelius, M.; Bernasconi, M.; Parrinello, M. *Phys. Rev. Lett.* **1997**, *78*, 2855.
- (12) Park, S. H.; Sposito, G. *Phys. Rev. Lett.* **2002**, *89*, 085501.
- (13) Spagnoli, C.; Loos, K.; Ulman, A.; Cowman, M. K. *J. Am. Chem. Soc.* **2003**, *125*, 7124.
- (14) Meleshyn, A. *J. Phys. Chem. C* **2008**, *112*, 14495.
- (15) Cheng, L.; Fenter, P.; Nagy, K. L.; Schlegel, M. L.; Sturchio, N. C. *Phys. Rev. Lett.* **2001**, *87*, 156103.
- (16) Fenter, P.; Sturchio, N. C. *Prog. Surf. Sci.* **2004**, *77*, 171.
- (17) Zhu, Y. X.; Granick, S. *Phys. Rev. Lett.* **2001**, *87*, 096104.
- (18) Xu, L.; Lio, A.; Hu, J.; Ogletree, D. F.; Salmeron, M. *J. Phys. Chem. B* **1998**, *102*, 540.
- (19) Park, C.; Fenter, P. A.; Nagy, K. L.; Sturchio, N. C. *Phys. Rev. Lett.* **2006**, *97*, 016101.
- (20) Hamley, I. W. *Angew. Chem., Int. Ed.* **2007**, *46*, 8128.
- (21) Lashuel, H. A.; LaBrenz, S. R.; Woo, L.; Serpell, L. C.; Kelly, J. W. *J. Am. Chem. Soc.* **2000**, *122*, 5262.
- (22) Zhang, S. *Nat. Biotechnol.* **2003**, *21*, 1171.
- (23) Zhang, F.; Du, H. N.; Zhang, Z. X.; Ji, L. N.; Li, H. T.; Tang, L.; Wang, H. B.; Fan, C. H.; Xu, H. J.; Zhang, Y.; Hu, J.; Hu, H. Y.; He, J. H. *Angew. Chem., Int. Ed.* **2006**, *45*, 3611.
- (24) Whitesides, G. M.; Grzybowski, B. *Science* **2002**, *295*, 2418.
- (25) Wu, Y.; Cheng, G.; Katsov, K.; Sides, S. W.; Wang, J.; Tang, J.; Fredrickson, G. H.; Moskovits, M.; Stucky, G. D. *Nat. Mater.* **2004**, *3*, 816.
- (26) Yu, B.; Sun, P.; Chen, T.; Jin, Q.; Ding, D.; Li, B.; Shi, A. C. *Phys. Rev. Lett.* **2006**, *96*, 138306.
- (27) Shin, K.; Xiang, H.; Moon, S. I.; Kim, T.; McCarthy, T. J.; Russell, T. P. *Science* **2004**, *306*, 76.
- (28) Kimmel, G. A.; Petrik, N. G.; Dohnalek, Z.; Kay, B. D. *Phys. Rev. Lett.* **2005**, *95*, 166102.
- (29) Kimmel, G. A.; Petrik, N. G.; Dohnalek, Z.; Kay, B. D. *J. Chem. Phys.* **2007**, *126*, 114702.
- (30) Hartgerink, J. D.; Granja, J. R.; Milligan, R. A.; Ghadiri, M. R. *J. Am. Chem. Soc.* **1996**, *118*, 43.
- (31) Wagner, D. E.; Phillips, C. L.; Ali, W. M.; Nybakken, G. E.; Crawford, E. D.; Schwab, A. D.; Smith, W. F.; Fairman, R. *Proc. Natl. Acad. Sci. U.S.A.* **2005**, *102*, 12656.
- (32) Li, B.; Zhang, Y.; Yan, S. H.; Lu, J. H.; Ye, M.; Li, M. Q.; Hu, J. *J. Am. Chem. Soc.* **2007**, *129*, 6668.
- (33) Cabiaux, V.; Brasseur, R.; Wattiez, R.; Falmagne, P.; Ruyschaert, J. M.; Goormaghtigh, E. *J. Biol. Chem.* **1989**, *264*, 4928.
- (34) Pratt, L. R.; Pohorille, A. *Chem. Rev.* **2002**, *102*, 2671.
- (35) Kowalewski, T.; Holtzman, D. M. *Proc. Natl. Acad. Sci. U.S.A.* **1999**, *96*, 3688.
- (36) Bellomo, E. G.; Wyrsta, M. D.; Pakstis, L.; Pochan, D. J.; Deming, T. J. *Nat. Mater.* **2004**, *3*, 244.
- (37) Ryadnov, M. G.; Woolfson, D. N. *Nat. Mater.* **2003**, *2*, 329.
- (38) Knowles, T. P.; Fitzpatrick, A. W.; Meehan, S.; Mott, H. R.; Vendruscolo, M.; Dobson, C. M.; Welland, M. E. *Science* **2007**, *318*, 1900.
- (39) Gawrisch, K.; Ruston, D.; Zimmerberg, J.; Parsegian, V. A.; Rand, R. P.; Fuller, N. *Biophys. J.* **1992**, *61*, 1213.
- (40) Zhang, L.; Wang, L.; Kao, Y. T.; Qiu, W.; Yang, Y.; Okobiah, O.; Zhong, D. *Proc. Natl. Acad. Sci. U.S.A.* **2007**, *104*, 18461.
- (41) Yang, D.-S.; Zewail, A. H. *Proc. Natl. Acad. Sci. U.S.A.* **2009**, *106*, 4122.
- (42) Whitesides, G. M.; Snyder, P. W.; Moustakas, D. T.; Mirica, K. A. Designing Ligands to Bind Tightly to Proteins. In *Physical Biology: From Atoms to Medicine*; Zewail, A. H., Ed.; Imperial College Press: London, 2008; pp 189.

JP903446G